MARTIN MARIETTA ENERGY SYSTEMS LIBRARIES
3 4456 0050749 5

CENTRAL RESEARCH LIBRARY
DOCUMENT COLLECTION

OAK RIDGE NATIONAL LABORATORY
operated by
UNION CARBIDE CORPORATION • NUCLEAR DIVISION
for the
U.S. ATOMIC ENERGY COMMISSION

ORNL-TM-3358

KINETIC MODELS FOR THE SYNTHESIS OF $(U,Pu)O_{2-y}$ BY HYDROGEN-REDUCTION AND CARBOTHERMIC TECHNIQUES

T. B. Lindemer and R. A. Bradley

OAK RIDGE NATIONAL LABORATORY
CENTRAL RESEARCH LIBRARY
DOCUMENT COLLECTION
LIBRARY LOAN COPY
DO NOT TRANSFER TO ANOTHER PERSON
If you wish someone else to see this document, send in name with document and the library will arrange a loan.
UCN-7969
(3 3-67)

NOTICE This document contains information of a preliminary nature and was prepared primarily for internal use at the Oak Ridge National Laboratory. It is subject to revision or correction and therefore does not represent a final report.

This report was prepared as an account of work sponsored by the United States Government. Neither the United States nor the United States Atomic Energy Commission, nor any of their employees, nor any of their contractors, subcontractors, or their employees, makes any warranty, express or implied, or assumes any legal liability or responsibility for the accuracy, completeness or usefulness of any information, apparatus, product or process disclosed, or represents that its use would not infringe privately owned rights.

ORNL-TM-3358

Contract No. W-7405-eng-26

METALS AND CERAMICS DIVISION

KINETIC MODELS FOR THE SYNTHESIS OF $(U,Pu)O_{2-y}$ BY HYDROGEN-REDUCTION AND CARBOTHERMIC TECHNIQUES

T. B. Lindemer and R. A. Bradley

Presented at the Annual Meeting of the American Ceramic Society, Chicago, Ill., April 24–29, 1971, and submitted to the Journal of Nuclear Materials

APRIL 1971

OAK RIDGE NATIONAL LABORATORY
Oak Ridge, Tennessee
operated by
UNION CARBIDE CORPORATION
for the
U.S. ATOMIC ENERGY COMMISSION

MARTIN MARIETTA ENERGY SYSTEMS LIBRARIES

3 4456 0050749 5

CONTENTS

Page

Abstract 1

1. Introduction 2

2. Kinetic and Thermodynamic Review 2

3. Hydrogen Reduction 6

3.1. Theory 6

3.2. Application to Experimental Data 9

4. Reduction Via the CO-CO_2-C System 14

4.1. Theory 14

4.2. Application to Experimental Data 24

5. Discussion and Conclusions 26

Acknowledgments 28

References 29

KINETIC MODELS FOR THE SYNTHESIS OF $(U,Pu)O_{2-y}$ BY HYDROGEN-REDUCTION AND CARBOTHERMIC TECHNIQUES

T. B. Lindemer and R. A. Bradley

ABSTRACT

Three models have been developed that permit the calculation of the time necessary for the synthesis of hypostoichiometric oxide from $(U,Pu)O_2$. The models are based on the interrelation between oxygen potential, valence of plutonium, and temperature determined by Rand and Markin and on the experimental conditions for reduction. Two reduction techniques are considered: the flowing hydrogen system and the $C-CO-CO_2$ system. At the usual temperatures for reduction, the partial pressure of water, the hydrogen flow, and the total weight of oxide are the most important factors in the hydrogen system, while in the $C-CO-CO_2$ system the important factors are the weight of the oxide in each oxide pellet, the partial pressure of carbon monoxide, the proximity of the oxide and the carbon used for reduction, and the minimum oxygen-to-metal ratio possible at the oxygen potential of the $C-CO-CO_2$ equilibrium.

1. Introduction

There are both advantages and disadvantages to the use of hypostoichiometric uranium-plutonium oxide in nuclear reactors. One principal advantage is improvement of the compatibility of the fuel and the cladding because the oxygen potential at certain stoichiometries is lower than that for the formation of many of the oxides of the metals present in the cladding material. In addition, since burnup results in the oxidation of the fuel, the use of hypostoichiometric oxide permits the accommodation of this burnup while maintaining a low oxygen potential. On the other hand, the attainment of low oxygen potentials in this system has caused considerable difficulty in the maintenance and control of the processes currently used for fabrication of the hypostoichiometric oxide.

This paper presents three mathematical models that permit the prediction of the time necessary for the attainment of a given hypostoichiometry. These developments are based in part on the thermodynamic data determined by Markin[1]) in the U-Pu-O system. This information is used to obtain the time dependence of the oxide stoichiometry for processes that employ hydrogen as a reductant. Additionally, the same thermodynamic information is used in the development of similar parameter interrelations for a second technique that utilizes the C-CO-CO_2 system for the reduction of the uranium-plutonium oxide.

2. Kinetic and Thermodynamic Review

The reduction of UO_2, U_4O_9, and U_3O_8 with hydrogen has been studied by several investigators. Lay[2]) reduced pellets of UO_{2+y} in hydrogen at

600 to 1100°C and concluded that the process was controlled by solid state diffusion of oxygen through the oxide to the pellet surface. He also determined that the chemical diffusion coefficient, $\tilde{D}$, of oxygen could be represented by

$$\tilde{D} = 0.5 \exp(-28{,}500/RT) \text{ cm}^2/\text{sec} \tag{1}$$

for the hyperstoichiometry range $0.003 < y < 0.08$. Other known studies[3–6]) reported the reduction of powders of uranium oxides in hydrogen at temperatures between 400 to 650°C; these reactions were controlled by a mechanism at the surface of the oxide particles. However, Lay's study at temperatures as low as 600°C indicated that a surface mechanism did not control the reduction of such massive oxide forms[2]). No studies of the kinetics of reduction of oxides in the U-Pu-O system have been reported.

The determination of the oxygen potentials, $RT \ln P_{O_2}$, by Markin[1]) for single-phase oxides containing 10 to 30% Pu is also important to the developments of this paper. These results were presented later by Rand and Markin[7]) in the form shown in fig. 1 for hypostoichiometric oxide. This figure illustrates that the oxygen potential is a function of valence and temperature alone. These data are, in turn, related to the oxygen-to-metal ratio (O/M) and the mole ratio $x = Pu/(U+Pu)$ by the expression

$$O/M = x\left(V_{Pu}/2\right) + (1 - x)\left(V_U/2\right); \quad \begin{array}{l} O/M < 2,\ V_U = 4 \\ O/M > 2,\ V_{Pu} = 4 \end{array} \tag{2}$$

in which the terms V_{Pu} and V_U represent the valence of plutonium and uranium, respectively. The oxygen potentials are also given in table 1

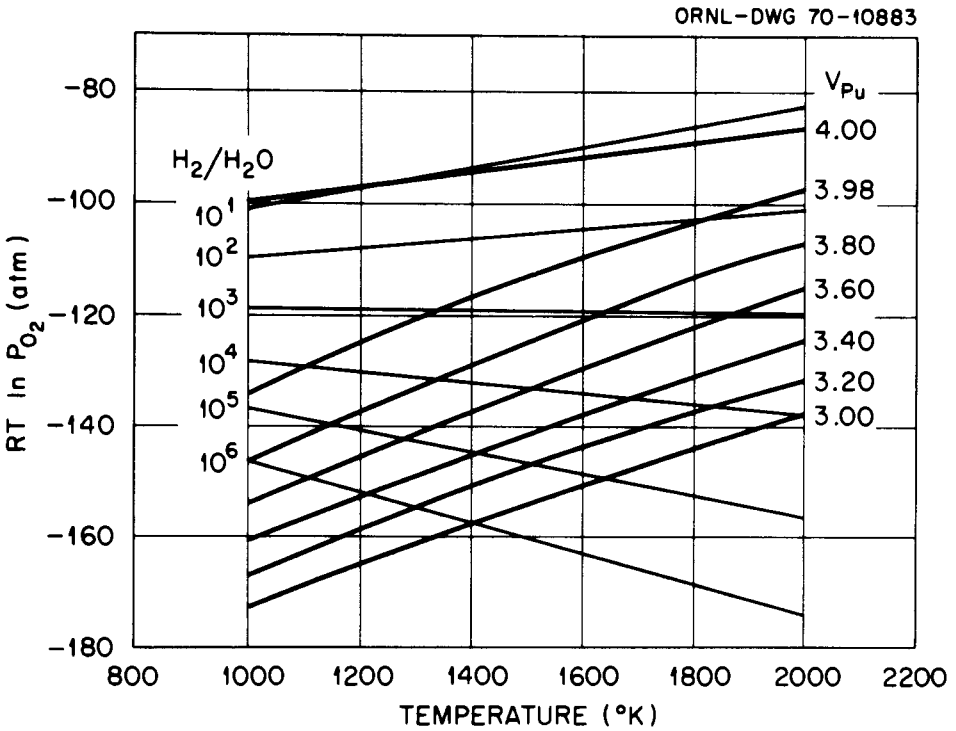

Fig. 1. Oxygen potential for $(U,Pu)O_{2-y}$ as a function of temperature for constant-valence and constant H_2/H_2O ratios.

Table 1. Oxygen potentials for $(U,Pu)O_{2-y}$ as a function of valence and temperature[a]

Valence		Oxygen Potential at $\underline{T}$(°K), kcal/mole $[-\underline{\Delta G}(O_2) = -\underline{RT}\ \ell n\underline{P}_{O_2}(atm)]$					
U	Pu	1000	1200	1400	1600	1800	2000
4.00	4.00	100	97	94.5	92	89.5	87
4.00	3.98	134	126	117.5	110	104	97.5
4.00	3.80	146.5	137.5	130	121	113	107
4.00	3.60	154	146	138	130	122.5	115
4.00	3.40	161	153	146	138	131.5	125
4.00	3.20	167	158.5	152	144	138	132
4.00	3.00	172.5	165	157.5	150.5	144	138

[a]Data taken from fig. 2 in: M. H. Rand and T. L. Markin, Thermodynamics of Nuclear Materials (IAEA, 1968), 637

as a function of temperature and valence; these values were obtained by Spear *et al.*[8]) from fig. 2 of Rand and Markin's paper[7]).

The oxygen potentials for $(U,Pu)O_{2-y}$ need to be converted to equivalent H_2/H_2O ratios for a later analysis of hydrogen-reduction techniques. Consider the reaction

$$2H_2O \rightleftharpoons 2H_2 + O_2 \tag{3}$$

for which one obtains

$$\ell n \frac{P_{H_2}}{P_{H_2O}} = \frac{-\left(\Delta G^\circ_T\right)_3 - RT\ \ell n P_{O_2}}{2RT} \tag{4}$$

where

$\underline{P}_{H_2}$, $\underline{P}_{H_2O}$, and $\underline{P}_{O_2}$ = pressure in atmospheres of the indicated gases,

$\underline{R}$ = 1.9869 cal/mole-°K,

$\underline{T}$ = temperature in °K,

$\left(\underline{\Delta G^\circ_T}\right)_3$ = standard free energy change of reaction (3) at temperature $\underline{T}$.

The value of $\left(\underline{\Delta G^\circ_T}\right)_3$ for reaction (3) at a given temperature was determined from the thermodynamic data found in the JANAF tables[9]) for water, hydrogen, and oxygen, and the value of the oxygen potential, $RT\ \ell n P_{O_2}$, was obtained from table 1. The particular value of the H_2/H_2O ratio was calculated and is given in table 2 as the log of the ratio. The temperature variation of the oxygen potential at given H_2/H_2O ratios was calculated in a similar manner and is shown in fig. 1.

Table 2. The value of log (H_2/H_2O)

Valence of Plutonium	Temperature, °K				
	1200	1400	1600	1800	2000
4.00	0.934	1.029	1.103	1.163	1.213
3.98	3.575	2.824	2.333	2.044	1.787
3.80	4.623	3.800	3.084	2.590	2.306
3.60	5.397	4.424	3.697	3.167	2.743
3.40	6.034	5.049	4.245	3.713	3.289
3.20	6.535	5.517	4.655	4.108	3.672
3.00	7.127	5.947	5.099	4.472	4.000

3. Hydrogen Reduction

The use of hydrogen to reduce the mixed oxide is the technique almost universally employed within the nuclear industry. Two different types of furnaces are commonly used – ceramic tube furnaces and furnaces employing refractory metal heating elements. The theoretical analysis to be developed below permits a prediction of the relation between O/M and reduction time in flowing hydrogen in such equipment.

3.1. Theory

The information outlined above was used to infer the probable controlling process in the hydrogen reduction of $(U,Pu)O_2$ pellets; from this a model was constructed for the reduction process. Three possibilities exist for process control: diffusion of oxygen to the surface of the pellet; a surface reaction; and the rate of removal of water by hydrogen flowing past the oxide. If we assume that reaction and transport in the mixed hypostoichiometric oxide are essentially the same as in UO_{2+y}, then Lay's observations[2]) eliminate control by the surface

reaction. Rand and Markin's data[7]) indicate that the H_2O/H_2 ratios are very small even for moderate hypostoichiometry, while the reverse situation exists for UO_{2+y}. This raises the possibility that attainment of hypostoichiometry may be controlled by the flow of hydrogen because the concentration of water in the gas is severely limited; in this case, the diffusion of oxygen in the pellet might not be limiting (i.e., diffusion would be sufficient to maintain complete saturation, in the thermodynamic sense, of the hydrogen). As will be shown later, this appears to be the case.

Consider the reaction involving an incremental flow-controlled reduction of the mixed oxide by dry (< 1 ppm water) hydrogen in a furnace maintained at a given temperature:

$$U_{1-x}Pu_xO_{2-y} + \Delta H_2 \rightarrow U_{1-x}Pu_xO_{2-y-\Delta} + \Delta H_2O \ . \qquad (5)$$

The most efficient use of the flowing hydrogen will be realized if the H_2/H_2O ratio of the effluent gas is that existing at the oxygen potential of the reduced oxide. For example, if this ratio were 100, then at optimum conditions 100 volumes of hydrogen would remove one volume of water from the system.

The increment of time required to accomplish the reduction in reaction (5) can be shown to be approximately

$$\Delta t = \frac{22.415\ N}{f_{H_2}}\ H\left(O/M_i - O/M_f\right) \qquad (6)$$

where

22.415 = liters per mole of gas at standard conditions,

$\underline{N}$ = moles of mixed oxide,

$\underline{f}_{H_2}$ = flow rate of hydrogen in liters per unit time at standard conditions,

$\underline{O}/\underline{M}_i$ = the O/M value prior to the incremental reduction,

$\underline{O}/\underline{M}_f$ = the O/M value after the incremental reduction,

$\underline{H}$ = the average H_2/H_2O ratio that exists during the incremental reduction.

The incremental change of the $\underline{O}/\underline{M}$ value was related more fundamentally to the change in valence of plutonium by differentiating the general relation between the $\underline{O}/\underline{M}$ and the valence of the uranium and plutonium in the system [eq. (2)] to give

$$O/M_i - O/M_f = \frac{x}{2}\left(V_{Pu_i} - V_{Pu_f}\right) \tag{7}$$

for hypostoichiometric oxide. By substituting eq. (7) into eq. (6) and applying the definition of a definite integral, the total time required to reduce stoichiometric oxide to a final $\underline{O}/\underline{M}$ value can be shown to be

$$t = 11.208 \frac{Nx}{f_{H_2}} \int_4^{V_{Pu}} H \, d\left(V_{Pu}\right) . \tag{8}$$

The value of the integral in eq. (8) was evaluated with the aid of a computer as a function of $\underline{V}_{Pu}$ at a given temperature. For the range $3.98 \leq \underline{V}_{Pu} \leq 4.00$, a linear relationship was assumed between $\ell n\underline{H}$ and $\underline{V}_{Pu}$ at each temperature shown in table 2. This was used to calculate in closed form the value of the integral at $\underline{V}_{Pu} = 3.98$. For the range $3.98 \geq \underline{V}_{Pu} \geq 3.00$, the variation of $\ell n\underline{H}$ with the values of $\underline{V}_{Pu}$ shown in

table 2 was approximated at each temperature with a least-squares polynomial of third degree; this polynomial always fitted the original data within a few percent. The values of $\underline{H}$ were generated at an increment of 0.01 in $\underline{V}_{Pu}$ and the integral evaluated via the trapezoidal rule at each increment of $\underline{V}_{Pu}$ to the final value of 3.00. The results of these calculations are summarized in fig. 2 and have been compared with similar manual calculations to ensure the accuracy of the procedure.

These results can also be used to calculate the times required to progress from one valence to another. For example, the time required for a reduction from $\underline{V}_{Pu} = 3.98$ to $\underline{V}_{Pu} = 3.94$ would be

$$t = 11.208 \frac{Nx}{f_{H_2}} \left[\int_4^{3.94} H \, d\left(V_{Pu}\right) - \int_4^{3.98} H \, d\left(V_{Pu}\right) \right] . \qquad (9)$$

3.2. Application to Experimental Data

Hypostoichiometric $(U,Pu)O_2$ pellets and sol-gel microspheres were prepared by heat treating the mixed oxide in a 3.2-cm-ID alumina tube furnace. The oxide pellets were prepared from mechanically mixed oxides containing < 100 ppm carbon. The reducing gas was Ar–4% H_2 containing less than 1 ppm water as it entered the furnace through a calibrated flowmeter and flowed over an open alumina boat that held the oxide, except as noted in table 3. A moisture monitor measured the water content of the effluent gas after it passed over the oxide. The heating and cooling rates were 300 and 450°C/h, respectively; during the cooling cycle the gas was changed to pure argon at 850°C. Descriptions of the material and heat-treatment conditions for several experiments are given in table 3.

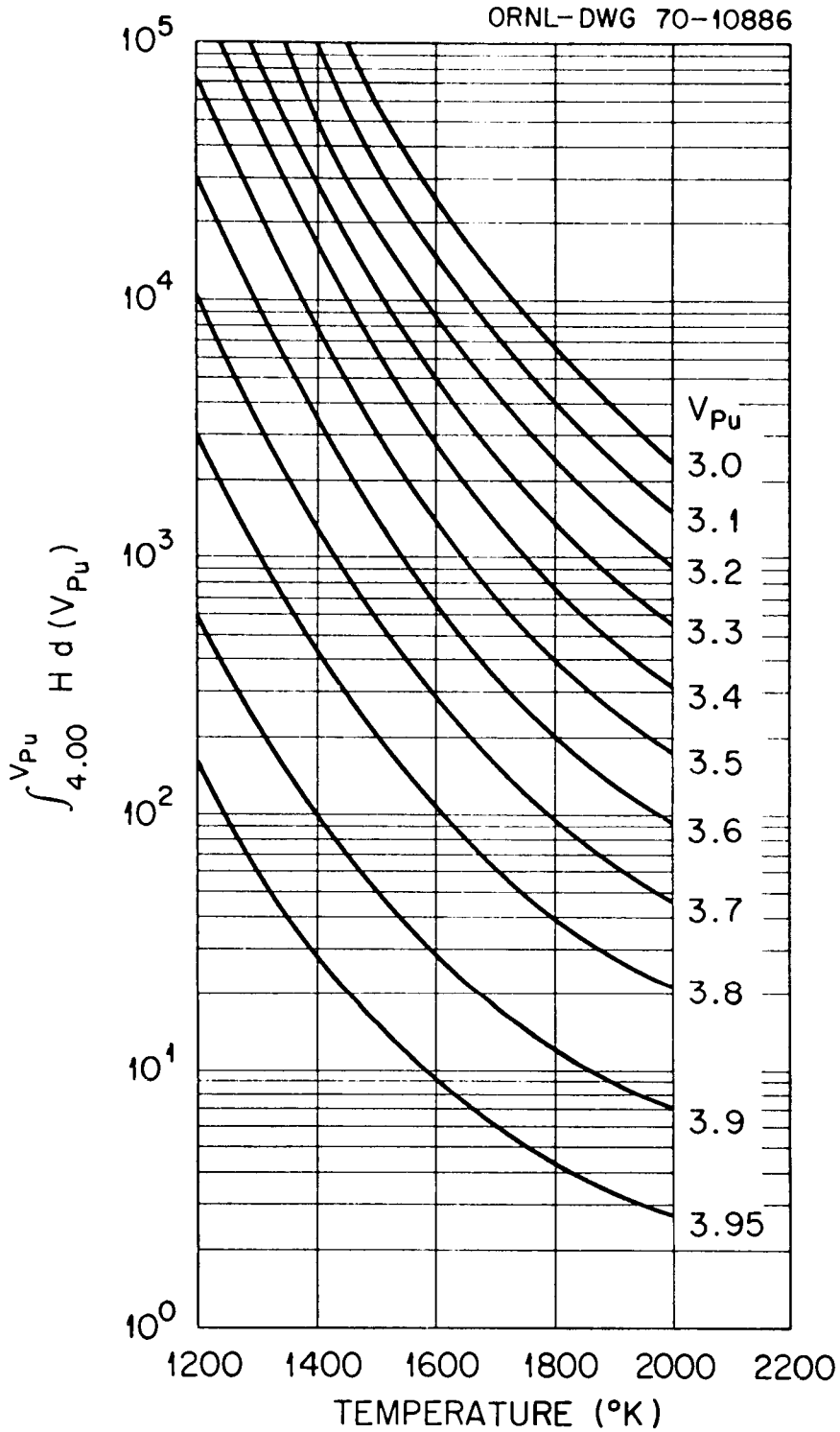

Fig. 2. The value of $\int_{4}^{V_{Pu}} \underline{H}\ \underline{d}\left(\underline{V}_{Pu}\right)$ as a function of temperature for constant valence $(U,Pu)O_{2-y}$.

Table 3. Experimental and predicted parameters for the hydrogen reduction of mixed oxides

Batch Number	Reference	Weight (g)	Pu/(U+Pu) (moles/mole)	Purge Gas	Gas Flow Rate (ft^3/h)	Temperature (°C)	Initial and Final O/M[a]	Time at Temperature per Kilogram of Mixed Oxide, h/kg		Predicted Time/ Actual Time	Remarks
								Actual	Predicted		
H164	This work	200	0.20	Ar–4% H_2	2.8	1400	1.988±0.005 1.956±0.005	500	1430	2.9	500 μm microspheres, < 100 ppm carbon Ar–4% H_2 passed through the bed
H165	This work	120	0.20	Ar–4% H_2	2.8	1400	2.000±0.002 1.965±0.005	237	783	3.3	< 44 μm microspheres, < 100 ppm carbon
H194	This work	109	0.25	Ar–4% H_2	2.8	1450	1.996±0.005 1.953±0.005	385	1679	4.4	0.493-cm-OD pellets, < 100 ppm carbon
Average of 8 runs H168–H178	This work	190	0.25	Ar–4% H_2	2.8	1450	2.000±0.002 1.974±0.004	31.6	200	6.3	500 μm microspheres, < 100 ppm carbon Ar–4% H_2 passed through the bed
Average of 4 runs H179–H182	This work	155	0.25	Ar–4% H_2	2.8	1450	2.000±0.002 1.982±0.004	45.2	97	2.1	< 44 μm microspheres, < 100 ppm carbon
Average of 25 runs FFTF pre-qualification	10	2000	0.25	N_2–6% H_2	18	1740	≈ 2.00 1.971±0.004	2	8.8	4.4	Carbowax 20M binder removed at 650°C in carbon dioxide for 1 h then 0.5 h in N_2–6% H_2. Carbon ≈ 65 ppm
WSA-3	11	500	0.25	Ar–5% H_2	4	1650	≈ 2.00 1.91	8	> 1000	> 125	1% Acrawax binder removed at 1000°C in Ar–5% H_2 for 1 h. Carbon ≈ 1600 ppm
Test sinters	12	≈ 100	0.25	Ar–8% H_2	8	1500	~ 1.94	40	230	5.75	2% Carbowax 20M binder removed at 675°C in dry helium for 3 h. Carbon unknown
PL-10-S11	12	4000	0.25	Ar–8% H_2	8	1500	1.990	1	5	5	2% Carbowax 20M binder removed at 675°C in dry helium for 3 h. Carbon unknown
PL-10-S13	12	254	0.25	Ar–8% H_2	8	1500	1.990 1.972	11.8	26	2.2	Previously sintered pellets. Carbon low
PL-10-S14	12	260	0.25	Ar–8% H_2	8	1650	1.990 1.962	11.5	33	2.9	Previously sintered pellets. Carbon low

[a]Errors are for 95% confidence interval about the mean.

The results of these experiments and several others reported in the literature[10–12]) were analyzed to determine the utility of eq. (9) in predicting the time required for the observed change in $\underline{O}/\underline{M}$. Comparisons of the actual times at temperature, normalized for a 1-kg batch, and the predicted times are shown in table 3. In all but one case, the ratio of the predicted time to the actual time is 4 ± 2. About half of the variation in this ratio can be accounted for by errors in the $\underline{O}/\underline{M}$ analyses; the remainder is probably due to differences in the configuration of the furnace systems. The large discrepancy between the predicted time and the actual time for batch WSA-3 can be attributed to the high carbon content after binder removal since the carbon would account for most of the reduction in $\underline{O}/\underline{M}$, as has been recognized by others[13]).

The experimental data show that a given $\underline{O}/\underline{M}$ is reached in a shorter time than would be predicted by eq. (9) even when the errors in oxygen-to-metal analyses are taken into account. This indicated that (a) either the values for $\underline{N}$, $\underline{x}$, or $\underline{f}_{H_2}$ in eq. (9) were wrong, or (b) the values of the integral given in fig. 2 were too high. The values used for $\underline{N}$, $\underline{x}$, and $\underline{f}_{H_2}$ were accurate since the weight of oxide, the ratio of Pu/(U+Pu), and the flow rate were known. The most reasonable assumption was that the values of the integral in fig. 2 were too high. This would result from the oxygen potential $\left(\underline{RT}\ \ell n\underline{P}_{O_2}\right)$ for a given $\underline{V}_{Pu}$ reported by Rand and Markin[7]) being too low. This is not unreasonable since their work was done at 1100°C and below and then extrapolated to higher temperatures.

The present results appear to be consistent with control of the process by the flow of hydrogen. The treatment by Crank[14]) of mass loss from solid spheres and cylinders under the conditions of the present

experiments shows that complete reduction takes place when $\tilde{D}t/a^2 \approx 1$. Since we knew both a, the radius of the body, and t, the experimental time (table 3), we approximated the minimum value of $\tilde{D}$, the chemical diffusion coefficient, necessary to transport oxygen out of the oxide at a rate sufficient to result in water saturation of the flowing hydrogen. These values ranged from 4.0×10^{-7} cm^2/sec for batch H194 to 1.9×10^{-10} cm^2/sec for batch H165. Additionally, upon assuming that Lay's results[2]) for UO_{2+y} approximated the behavior of the hypostoichiometric mixed oxide, eq. (1) was used to calculate a value of $\tilde{D}$ of about 2×10^{-4} cm^2/sec at the temperatures of the present experiments. This value is at least three orders of magnitude higher than those calculated above. Additionally, Lay's work[2]) eliminated control by a reaction at the gas-oxide interface for massive oxide forms. One would therefore conclude that the reduction is most likely controlled by removal of water via the flow of reducing gas in the present experiments. This is consistent with the assumptions that led to eq. (9) and the reasonable agreement between observed and predicted O/M values obtained through the use of eq. (9) as shown in table 3.

The use of nitrogen-hydrogen mixtures for reduction may lead to solid-solution nitrogen in the mixed oxide, fluorite lattice. The use of these mixtures is occasionally reported in the literature[10,15,16]). Recent work on the U-O-N system by Benz *et al.*[17]), Blum *et al.*[18]), and Martin[19]) demonstrated an extensive solid-solution region between UO_2 and U_2N_3 at the temperatures normally used for reduction of the mixed oxide. Such a solution in the mixed oxide was indicated in table 12-4 of reference 15, where 2500 ppm of chemically combined nitrogen was

found in oxide having an O/M of 1.94. The presence of nitrogen in the fuel would probably result in errors in the O/M values determined by the usual gravimetric techniques and would complicate the interpretation of possible interactions between the fuel and the cladding during irradiation.

4. Reduction Via the CO-CO_2-C System

Uranium-plutonium oxide can be reduced by carbon monoxide in the presence of carbon in a way that is different from the system that involves flowing hydrogen. Essentially, the basic features of this technique require an intimate association of each oxide form with free carbon in an atmosphere that contains sufficient carbon monoxide to suppress the carbide-forming reactions. This process is not applicable to refractory metal furnaces because the C-CO-CO_2 system would cause carburization of the refractory metal.

4.1. Theory

4.1.1. Thermodynamics

The CO-CO_2-C system is capable of establishing oxygen potentials that are within the range of those necessary for a V_{Pu} as low as 3.00. These potentials were calculated by considering first the equilibrium reaction

$$C + CO_2 \rightleftharpoons 2CO \ . \tag{10}$$

The expression for the equilibrium constant was written in the form

$$\left(K_{eq}\right)_{10} = P_{CO}\left(\frac{P_{CO}}{P_{CO_2}}\right) \tag{11}$$

for unit activity of carbon. Also, the oxygen pressure is established via the reaction

$$2CO + O_2 \rightleftharpoons 2CO_2 \tag{12}$$

for which one obtains

$$\left(K_{eq}\right)_{12} = \exp\left[\left(-\Delta G_T^\circ\right)_{12} \Big/ RT\right] = \left(\frac{P_{CO_2}}{P_{CO}}\right)^2 \frac{1}{P_{O_2}} \ . \tag{13}$$

From eqs. (11) and (13) it follows that

$$RT\ \ell n\ P_{O_2} = \left(\Delta G_T^\circ\right)_{12} - 2RT\ \ell n\left[\left(K_{eq}\right)_{10} \Big/ P_{CO}\right] \ . \tag{14}$$

Equation (14) was used along with the thermodynamic data in the JANAF tables[9]) for C, CO, and CO_2 to calculate the dependence of the oxygen potential on the temperature and pressure of carbon monoxide. The results are shown in fig. 3 along with the results of Rand and Markin[7]). Also shown are the approximate maximum oxygen potentials that exist during the formation of carbides from the oxides; these were determined from the equilibrium pressures of carbon monoxide for the UO_2-CO-C-$UC_{1.86}$ and the Al_2O_3-C-CO-Al_4C_3 systems and eq. (14). The free energy functions used in these calculations were obtained from Leitnaker and Godfrey[20]) for UO_2 and $UC_{1.86}$ and from the JANAF tables[9]) for the other materials.

Several features are clear from a consideration of fig. 3: (1) carbides will not form from the mixed oxide of the alumina furnace tube at the temperatures and pressures of carbon monoxide where it is possible to obtain hypostoichiometric oxide; (2) the temperatures and

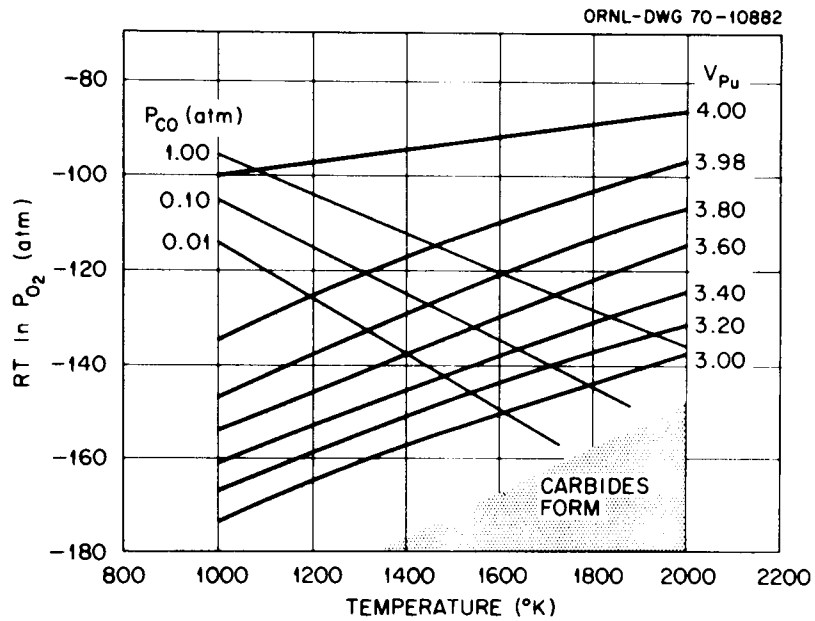

Fig. 3. Oxygen potential for $(U,Pu)O_{2-y}$ as a function of temperature for constant valence and for the C-CO-CO_2 equilibrium at indicated pressures of carbon monoxide.

the pressure of carbon monoxide can be varied over a wide range to obtain a given oxygen potential; (3) the placement of the uranium-plutonium oxide in an environment maintained at the equilibrium of the CO-CO_2-C system results in the ultimate establishment by this equilibrium of a minimum and predictable oxygen potential in the oxide. Consequently, by suitably controlling the temperature and the pressure of carbon monoxide, a given O/M can be established in the oxide.

4.1.2. Kinetic Models

Two kinetic models were developed to predict the minimum time necessary to achieve a given O/M value greater than or equal to that of the final equilibrium value. Two models were necessary because the experimental results indicated that the rate-controlling process depended on

the physical arrangement of the reactants during the reduction process. Consider a physical system in which the surface of an oxide body faces a carbon surface across an incremental distance, $\underline{\Delta Z}$. The gap between the two surfaces is filled with a gas containing a given pressure of carbon monoxide. The following assumptions are also made for both models:

1. The CO/CO_2 ratio at the surface of the oxide body is that which exists at the $\underline{O}/\underline{M}$ (i.e., oxygen potential) of the entire oxide body.
2. The solid-state diffusion of oxygen in the oxide does not control the reaction. This is a reasonable assumption in view of the results from the hydrogen-reduction experiment discussed earlier.
3. The postulated reaction at the surface of the oxide pellet,

$$U_{1-x}Pu_xO_{2-y} + \Delta CO \rightleftharpoons \Delta CO_2 + U_{1-x}Pu_xO_{2-y-\Delta} , \qquad (15)$$

does not control the reaction.

The first kinetic model can now be developed. It is based on the additional assumptions that:

4. The reaction at the surface of the carbon [eq. (10)] does not control the reaction.
5. The CO/CO_2 ratio at the carbon surface is that for the $C\text{-}CO\text{-}CO_2$ equilibrium.
6. The reduction is controlled by the diffusion of carbon dioxide, which is produced via reaction (15), from the oxide surface to the carbon surface.

This reduction proceeds as long as the CO/CO_2 ratio at the oxide surface is less than that established by the equilibrium of reaction (10). For the incremental reaction (15), and again using eq. (7), the expression for the moles of carbon dioxide produced, $\underline{N}_{CO_2}$, is

$$N_{CO_2} = \frac{v\left(O/M_i - O/M_f\right)}{\theta} = \frac{vx\left(V_{Pu_i} - V_{Pu_f}\right)}{2\theta} , \qquad (16)$$

in which $\underline{v}$ is the volume of the oxide body and $\underline{\theta}$ is the molar volume of the oxide, ≈ 24.6 cm^3/mole. This is set equal to the flux of carbon dioxide, $\underline{J}_{CO_2}$, across the incremental distance $\underline{\Delta Z}$, in the increment of time, $\underline{\Delta t}$,

$$N_{CO_2} = J_{CO_2}\ A\Delta t = -\frac{\left(P\tilde{D}_{12}\right)}{RT}\ \frac{\left(X - X_c\right)_{CO_2}}{\Delta Z}\ A\Delta t , \qquad (17)$$

where

$\underline{R}$ = 82.06 cm^3-atm/mole °K,

$\underline{A}$ = geometrical surface area in cm^2 of the oxide body,

$\frac{\left(X - X_c\right)_{CO_2}}{\Delta Z}$ = average concentration gradient of CO_2 in mole fraction per cm existing between the oxide and the carbon surfaces during the incremental change in $\underline{V}_{Pu}$,

$\underline{P\tilde{D}}_{12}$ = a pressure-independent quantity that has the units atm·cm^2/sec and that is the product of the total pressure, $\underline{P}$, in the system and the interdiffusion coefficient, $\underline{\tilde{D}}_{12}$, of carbon dioxide in the solvent gas[21]).

By equating eqs. (16) and (17) and summing over all incremental times, the equation for the time to reduce the oxide from an $\underline{O/M}$ of 2.00 can be shown to be

$$t(h) = \frac{xv\ \Delta Z\ RT}{A\ 7200\left(P\tilde{D}_{12}\right)\theta} \int_4^{V_{Pu}} \frac{1}{\left(X - X_c\right)_{CO_2}}\ d\left(V_{Pu}\right) . \qquad (18)$$

Since the concentration gradient has been maximized via assumptions (1) and (5), eq. (18) gives a minimum theoretical time necessary for the reduction.

Inherent in eq. (18) is a dependence on the pressure of carbon monoxide in the gas mixtures. That is, at a given oxygen potential there exists a given CO/CO_2 ratio, and it follows that the mole fraction of carbon dioxide present is directly dependent on the pressure of carbon monoxide. Correspondingly, eq. (18) was rearranged to give

$$t = \frac{xv\ \Delta Z\ RTP}{A\ 7200\left(P\tilde{D}_{12}\right)\theta P_{CO}} \int_{4}^{V_{Pu}} \left[\frac{1}{r} - \frac{1}{r_c}\right]^{-1} d\left(V_{Pu}\right) \tag{19}$$

or

$$t = \frac{xv\ \Delta Z}{A} F\left(V_{Pu}\right) \tag{19a}$$

where

$$F\left(V_{Pu}\right) \equiv \frac{RTP}{7200\left(P\tilde{D}_{12}\right)\theta P_{CO}} \int_{4}^{V_{Pu}} \left[\frac{1}{r} - \frac{1}{r_c}\right]^{-1} d\left(V_{Pu}\right) \tag{19b}$$

in which $\underline{P}_{CO}$ is the partial pressure of carbon monoxide and $\underline{r}$ and $\underline{r}_c$ are the CO/CO_2 ratios that correspond to $\underline{X}$ and $\underline{X}_c$, respectively. As will be seen, the integral in eq. (19) was easier to evaluate numerically than was that in eq. (18).

The effect of process variables on the experimental time can be inferred from eq. (19a). At a given temperature the time can be reduced by bringing the carbon and the oxide into very close proximity, thus minimizing $\underline{\Delta Z}$. Also, the time is dependent only on the volume-to-area

ratio of the individual oxide body and is independent of the total number of oxide bodies being reduced in the furnace as long as each is surrounded by carbon. By contrast, the time for the hydrogen process [eq. (8)] is dependent on the total weight of oxide present in the furnace. Increasing the relative pressure of carbon monoxide in the gas mixture decreases the time for the reduction; the use of 100% carbon monoxide results in the minimum time. Unlike the hydrogen-reduction process, no flow of gas is required other than that necessary to prevent a gross change in the carbon monoxide pressure as the reduction proceeds via reaction (15).

The value of $\underline{F}\left(\underline{V}_{Pu}\right)$ in eq. (19b) was evaluated in a manner essentially identical to that used for eq. (8). The value of a particular CO/CO_2 ratio (i.e., $\underline{r}$) was obtained from the H_2/H_2O ratio at a given $\underline{V}_{Pu}$ by considering the reaction

$$H_2 + CO_2 \rightleftharpoons CO + H_2O \tag{20}$$

for which one obtains the relation

$$\left(K_{eq}\right)_{20} \frac{P_{H_2}}{P_{H_2O}} = \frac{P_{CO}}{P_{CO_2}} \quad . \tag{21}$$

The value of $\left(K_{eq}\right)_{20}$ was determined from the thermodynamic data in the JANAF tables[9]); in order to obtain $\underline{r}$, this was multiplied by the value of the H_2/H_2O ratio generated from the curve-fitting routines described in section 3.1. The average value of $1/\underline{r}$ was calculated for the incremental range of $\underline{V}_{Pu}$ and the value of $1/\underline{r}_f$ was calculated from eq. (14) for the final equilibrium oxygen potential at a given temperature

and pressure of carbon monoxide. These values then permitted the evaluation of the integral. The value of the integral was multiplied by $\underline{RTP}/7200 \left(\underline{P\tilde{D}}_{12}\right) \underline{\theta P}_{CO}$, which is constant at a given temperature and pressure of carbon monoxide, to give $\underline{F}\left(\underline{V}_{Pu}\right)$. Two different sets of calculations were made, one for an Ar–10% CO gas mixture and another for 100% carbon monoxide at 1.0 atm. For the Ar-CO gas mixture the product, $\underline{P\tilde{D}}_{12}$, was obtained from the general relationship

$$\ell n \left(P\tilde{D}_{12}\right) = \ell n\alpha + s\ \ell nT - S/T \tag{22}$$

in which $\underline{\alpha} = 1.74 \times 10^{-5}$ atm·cm^2/sec (°K)^s, $\underline{s} = 1.646$, and $\underline{S} = 89.1$°K, while for interdiffusion in CO-CO_2 mixtures, the numerical values are $\underline{\alpha} = 0.577 \times 10^{-5}$, $\underline{s} = 1.803$, and $\underline{S} = 0$ (table 7, reference 21). The values of $\underline{P\tilde{D}}_{12}$ in the two systems are accurate within 15% and differ from each other by only about 10% in the temperature range of interest and are independent of carbon dioxide concentration within the quoted limit of accuracy[21]). The values of $\underline{F}\left(\underline{V}_{Pu}\right)$ are given in figs. 4 and 5. The dashed boundary at the upper left represents the transition from kinetic to thermodynamic control; values of $\underline{F}\left(\underline{V}_{Pu}\right)$ above the boundary are meaningless because the oxide is in equilibrium with carbon, carbon monoxide, and carbon dioxide and will not reduce further.

The second kinetic model for the reduction of the oxide by carbon is based on control by the rate of reaction (10). Assumptions 1, 2, and 3 still hold and the diffusion of carbon dioxide in assumption (6) is now not controlling. There is general agreement in the literature that the rate of the reaction of carbon dioxide with carbon can be represented by the expression

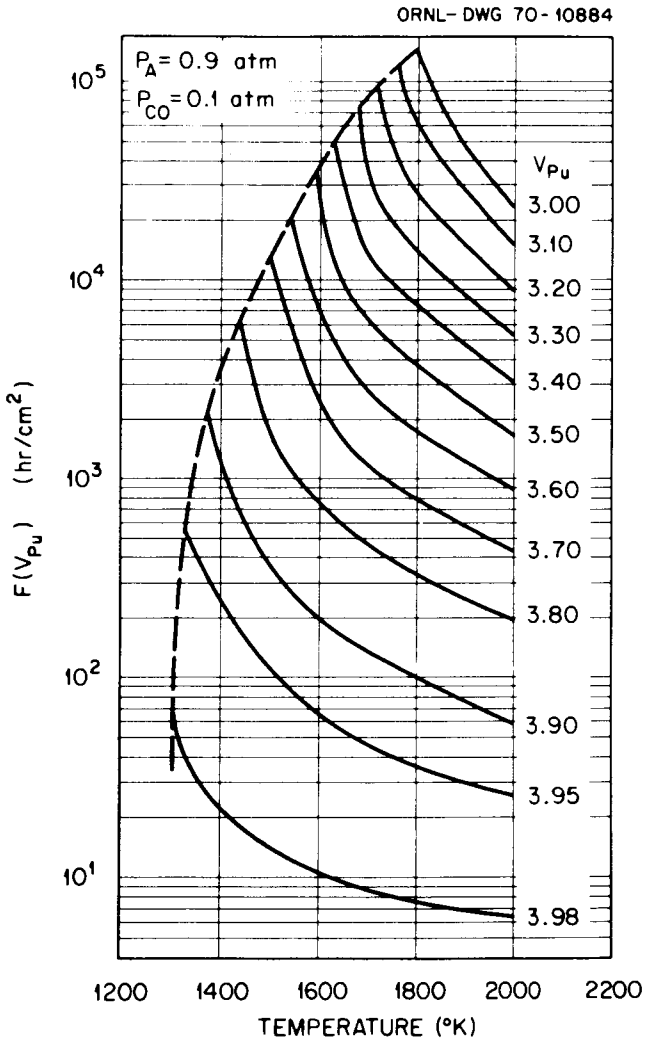

Fig. 4. The value of $\underline{F}\left(\underline{V}_{Pu}\right)$ as a function of temperature for constant-valence $(U,Pu)O_{2-y}$ and an Ar–10% CO gas mixture at a pressure of 1 atm.

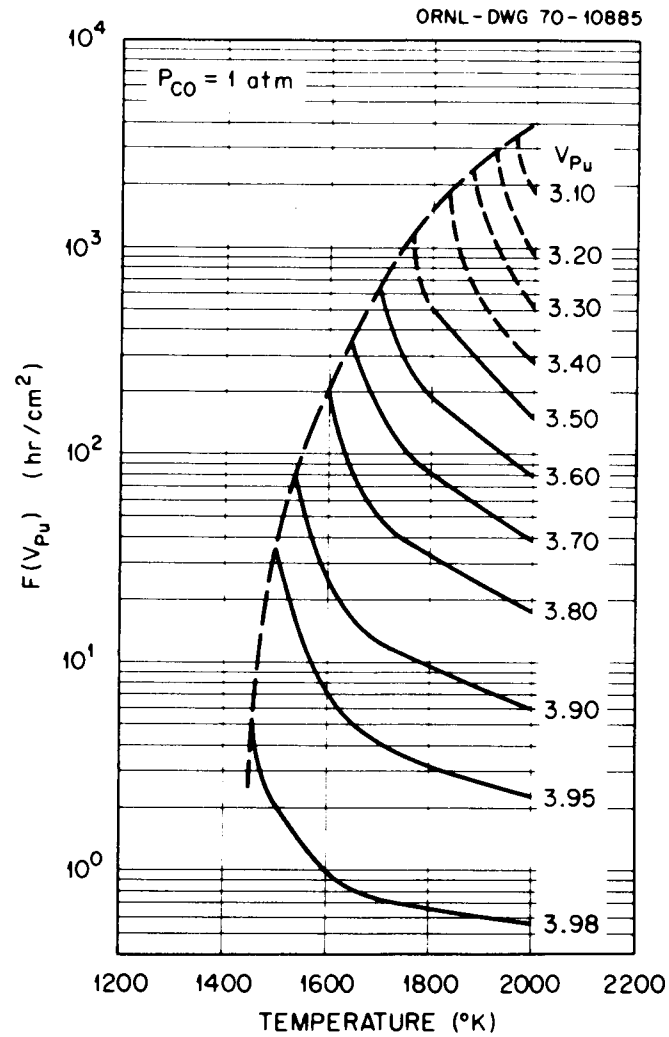

Fig. 5. The value of $\underline{F}\left(\underline{V}_{Pu}\right)$ as a function of temperature for constant-valence $(U,Pu)O_{2-y}$ for carbon monoxide at a pressure of 1 atm.

$$\text{rate} = \frac{k_1 P_{CO_2}}{1 + k_2 P_{CO} + k_3 P_{CO_2}} \left[\frac{\text{g-mole } CO_2}{\text{min}\cdot\text{atm}}\right] \tag{23}$$

in which $\underline{k}_1$, $\underline{k}_2$, and $\underline{k}_3$ are temperature-dependent rate constants[22]. At the pressures and temperatures of the present experiments, the results in the literature[22-24] demonstrate that $\underline{k}_3\underline{P}_{CO_2} \ll \underline{k}_2\underline{P}_{CO} < 1$ and that $\underline{k}_1 = \underline{k}_{10} \exp(-59{,}000/RT)$. The increment of time for the incremental reduction of reaction (15) can be shown to be

$$\Delta t = \frac{vx \exp(59{,}000/RT) \left(P_{CO}/P_{CO_2}\right)}{2k_{10}\ \theta P_{CO}} \left(V_{Pu_i} - V_{Pu_f}\right) \tag{24}$$

in which the CO/CO_2 ratio is that in equilibrium with the oxide during the incremental reduction. Upon integration, the expression for the time necessary to reduce to a given $\underline{O}/\underline{M}$ value becomes

$$t = \frac{vx \exp(59{,}000/RT)}{2k_{10}\ \theta P_{CO}} \left(k_{eq}\right)_{20} \int_4^{V_{Pu}} H\, d\left(V_{Pu}\right) \tag{25}$$

The value of $\underline{k}_{10}$ is the only unknown quantity in this expression; it can be determined from a set of initial reductions. The literature results indicate that $\underline{k}_{10}$ may be sensitive to factors such as the type of carbon used, the surface area of the carbon, and, in the present use, the experimental ratio of oxide to carbon. Therefore, these factors should be kept constant. Equation (25) indicates that the reduction is proportional only to the volume of oxide in the individual oxide body, again indicating a possible advantage of this process over that of flowing hydrogen.

4.2. Application to Experimental Data

A test of the carbon reduction method was made in four experimental runs in the same alumina tube furnace used for hydrogen reduction. A 2.5-cm-OD × 5.0-cm-long carbon cylinder was split lengthwise, and six 0.635-cm-diam × 0.635-cm-deep holes were drilled in each half so that the holes were aligned when the cylinder was reassembled. Six 90%-dense, 0.50-cm-OD × 0.56- to 0.58-cm-long $(U_{0.75}Pu_{0.25})O_2$ pellets containing < 100 ppm carbon were placed in the block, one in each set of matching holes. This block was placed in the furnace and an Ar–10% CO mixture passed through the furnace at 0.5 liter/min so that the partial pressure of carbon monoxide in the furnace remained reasonably constant during the reduction. The same heating and cooling rates used in the hydrogen reductions were used, with treatments being performed at 1350, 1450, and 1550°C for 8 h and at 1450°C for 62 h. The experimental $\underline{O}/\underline{M}$ values and the corresponding values of $\underline{V}_{Pu}$ for the reduced oxide are shown in table 4; analyses showed no increase in carbon content during treatment.

The predicted times for the carbon dioxide diffusion model were calculated from eq. (19a) and the experimental values of $\underline{V}_{Pu}$, $\underline{A}$, $\underline{x}$, $\underline{v}$, and $\underline{\Delta Z}$. It was assumed that only the bottom face and the sides of the pellet were included in the area of the pellet, since the top face was not near a carbon surface, and that the oxide-carbon gap at the bottom of the pellet, which rested on the conical face of the drilled hole, was the same as the radial gap. The predicted times were calculated from the expression

Table 4. Observed and calculated times for reduction of $(U_{0.75}Pu_{0.25})O_2$ in the C-CO-CO_2 system

Temperature (°C)	t_{obs} (h)	$\underline{O}/\underline{M}_{obs}$	V_{Pu}	Eq. (19a)			Eq. (25)			
				$F\left(V_{Pu}\right)$ (h/cm^2)	t_{19a} (h)	t_{obs}/t_{19a}	$\left(K_{eq}\right)_{20}$	$\int H\, d\left(V_{Pu}\right)$	t_{25} (h)	t_{obs}/t_{25}
1350	8	1.979	3.82	500	0.90	8.90	3.07	54	6.9	0.86
1450	8	1.960	3.68	1250	2.24	3.57	3.48	160	8.0	1
1450	62	1.943	3.54	3900	7.00	8.86	3.48	470	23.5	0.38
1550	8	1.930	3.44	5000	8.97	0.89	3.86	510	9.7	1.22

$$t = \frac{x\ ah\ \Delta Z\ F\left(V_{Pu}\right)}{(a + 2h)} = \frac{0.25(0.25)0.57(0.07)\ F\left(V_{Pu}\right)}{(0.25 + 1.14)}\ , \qquad (26)$$

in which $\underline{a}$ is the radius of the pellet and $\underline{h}$ the height; $\underline{F}\left(\underline{V}_{Pu}\right)$ was determined from the experimental temperature and $\underline{O}/\underline{M}$ value [eq. (2)] and fig. 4. These predicted times and the other quantities used in the calculations are shown in table 4. As can be seen from the table, the agreement is good only at 1550°C.

The predicted times for the model based on the CO_2-C reaction were calculated from the same experimental results. The value of $\underline{k}_{10}$ was calculated from eq. (25) and the results at 8 h and 1450°C; it was 1.95×10^5 g-mole CO_2/min·atm. This value was then used to calculate the predicted times for the three other experimental runs. The results shown in table 4 indicate that the reaction of carbon dioxide with carbon was controlling the reaction at the lower two temperatures. The predicted times calculated from either eq. (25) or eq. (26) indicate that the reduction rates at 1550°C are equivalent for either mechanism for our particular experimental arrangement.

5. Discussion and Conclusions

A direct comparison of the times necessary for reduction to a given $\underline{O}/\underline{M}$ with the hydrogen and C-CO-CO_2 systems is instructive. Assume the reduction of one kilogram of $(U_{0.75}Pu_{0.25})O_{2.00}$ in the form of 0.635-cm-diam × 0.635-cm-long pellets at 1650°C. In the hydrogen system also assume a total gas flow of 18 ft^3/h of either Ar–8% H_2 or pure hydrogen, while in the C-CO-CO_2 system assume a gap distance, $\underline{\Delta Z}$, of 0.07 cm and a gas mixture of Ar–10% CO. Equations (8), (19a), or (25) were used to

calculate the times for reduction shown in table 5. The calculated results from eq. (8) include the factor of ≈ 0.25 observed to be necessary to arrive at the correct predicted time; the calculations from eq. (25) should be directly comparable to those of eq. (8) since the value of $\underline{k}_{10}$ was determined from experimental data, while no such correction was made to the results from eq. (19a). The calculations for the hydrogen system clearly show that the use of Ar–8% H_2 results in unacceptably long reduction times when $\underline{O}/\underline{M}$ values below 1.94 are desired; the use of pure hydrogen results in more reasonable times. The calculations for an Ar–10% CO gas mixture in the C-CO-CO_2 system demonstrate that the use of this system results in experimental times that are comparable to flowing hydrogen and are clearly superior to flowing Ar–8% H_2.

A comparison of the experimental and extrapolated times for reduction of $(U,Pu)O_2$ shown in table 3 indicate that the extrapolated oxygen potentials of Rand and Markin[7]) are too low for a given valence of plutonium.

Table 5. Calculated times to reduce $(U_{0.75}Pu_{0.25})O_2$ pellets to given $\underline{O}/\underline{M}$ values at 1650°C

Oxygen-to-Metal Ratio	Valence of Plutonium	Time in Given Atmosphere, h			
		Ar–8% H_2	Hydrogen	Ar–10% CO	
		0.25 × Eq. (8)		Eq. (19a)	Eq. (25)
1.98	3.84	1.0	0.10	0.30	0.37
1.96	3.68	4.3	0.35	1.2	1.6
1.94	3.52	13	1.0	3.7	4.6
1.92	3.36	33	2.8	10	12.0
1.90	3.20	83	6.8	26	30.0

The models developed in this paper permit the correlation of the experimental parameters for the reduction of $(U,Pu)O_2$. At a given temperature and plutonia content, the following factors are most important:

H_2 system

1. the total weight of oxide to be reduced
2. the flow of hydrogen through the system
3. the partial pressure of water

C-CO-CO_2 system

1. the weight of oxide in each oxide pellet or microsphere
2. the partial pressure of CO
3. the minimum O/M possible at the C-CO-CO_2 equilibrium
4. the proximity of the oxide and the carbon

For a given set of conditions in the latter system, the actual time for reduction will be the longer of the two times calculated from eqs. (19a) and (25) because the controlling process is the one having the slower rate. These models thus permit the selection of a reduction system that meets particular processing requirements.

Acknowledgments

The authors wish to thank K. E. Spear for suggesting the relevance of the thermodynamic properties of $(U,Pu)O_{2-y}$ to the reduction processes. We also thank A. P. Malinauskas and W. J. Lackey for their helpful discussions, W. B. Stines and W. H. Miller for their assistance with the experimental work, and J. H. Cooper for the chemical analysis.

References

1) T. L. Markin, Chem. Eng. Progr. Symp. Ser. 80 (1967) 43

2) K. W. Lay, J. Am. Ceram. Soc. 53 (1970) 369

3) V. G. Vlasov, V. T. Pis'menko, and A. A. Larin, Kinetika i Kataliz 9 (1968) 1094; English translation, 901

4) V. G. Vlasov, V. T. Pis'menko, and A. A. Larin, Zh. Prik. Khim. 41 (1968) 2640; English translation, 2487

5) V. T. Pis'menko, V. G. Vlasov, and A. A. Larin, Kinetika i Kataliz 10 (1969) 203; English translation, 164

6) S. Aronson and J. L. Clayton, J. Inorg. Nucl. Chem. 7 (1958) 384

7) M. H. Rand and T. L. Markin, Thermodynamics of Nuclear Materials, (IAEA, 1968), 637

8) K. E. Spear, A. R. Olsen, and J. M. Leitnaker, ORNL (USA) Report TM-2494 (1969)

9) JANAF Thermochemical Tables (Dow Chemical Company, Midland, Michigan, 1968)

10) L. J. Ferrell, D. L. Fowler, C. R. Sherman, and J. M. Kerr, Bull. Am. Ceram. Soc. 49 (1970) 448

11) M. G. Bale, B. Riley, T. W. Wallace, and N. G. Wolcott, Jr., WARD (USA) Report 4135-11 (1970) 11-3, 12-3

12) H. T. Blair, BNWL (USA) Report 1214 (1970)

13) H. T. Blair and J. E. Samis, WHAN (USA) Report IR-2 (1970) 8.3

14) J. Crank, The Mathematics of Diffusion (Oxford University Press, London, 1956) 72, 90

15) J. Y. Chang, P. M. French, W. R. Jacoby, and P. D. Shalek, WARD (USA) Report 4135-11 (1970) 12-4

16) M. Kurihara, J. Abe, S. Fukushima, T. Sasayama, and J. Shimokawa, Plutonium 1970 and Other Actinides, Nuclear Metallurgy 17, Part I (AIME, New York, 1970) 84

17) R. Benz, G. Balog, and B. H. Baca, High Temp. Sci. 2 (1970) 221

18) P. L. Blum, J. Laugier, and J. M. Martin, C. R. Acad. Sc. Paris, Ser. C 268 (1969) 148

19) J. M. Martin, J. Nucl. Mater. 34 (1970) 81

20) J. M. Leitnaker and T. G. Godfrey, J. Chem. Eng. Data 11 (1966) 392

21) E. A. Mason and T. R. Marrero, Advances in Atomic and Molecular Physics 6 (Academic Press, New York, 1970) p. 155

22) A. E. Reif, J. Phys. Chem. 56 (1952) 785

23) S. Ergun, J. Phys. Chem. 60 (1956) 480

24) I. L. Mar'yasim and P. A. Tesner, Dok. Akad. Nauk SSSR 163 (1965) 1430; English translation, 622

INTERNAL DISTRIBUTION

1–3. Central Research Library
4. ORNL – Y-12 Technical Library Document Reference Section
5–14. Laboratory Records Department
15. Laboratory Records, ORNL RC
16. ORNL Patent Office
17. G. M. Adamson, Jr.
18–22. R. A. Bradley
23. R. E. Brooksbank
24. J. V. Cathcart
25. J. H. Coobs
26. C. M. Cox
27. F. L. Culler, Jr.
28. J. E. Cunningham
29. H. J. de Nordwall
30. D. E. Ferguson
31. R. B. Fitts
32. J. H Frye, Jr.
33. W. R. Grimes
34. P. A. Haas
35. R. G. Haire
36. W. O. Harms
37–39. M. R. Hill
40–86. P. R. Kasten
87. W. J. Lackey
88. J. M. Leitnaker
89. R. E. Leuze
90–94. T. B. Lindemer
95. A. L. Lotts
96. T. S. Lundy
97. A. P. Malinauskas
98. K. H. McCorkle
99. W. T. McDuffee
100. C. J. McHargue
101. K. J. Notz
102. A. R. Olsen
103. J. R. Parrott
104. P. Patriarca
105. J. L. Scott
106. J. D. Sease
107. R. E. Thoma
108. D. B. Trauger
109. J. R. Weir
110. R. G. Wymer
111. C. S. Yust

EXTERNAL DISTRIBUTION

DIVISION OF REACTOR DEVELOPMENT AND TECHNOLOGY, AEC, Washington

112. E. E. Kintner
113. E. C. Norman
114. S. Rosen
115–116. J. M. Simmons

AEC-RDT SITE REPRESENTATIVES

117. M. E. Jackson, Argonne National Laboratory
118. R. L. Morgan, Atomics International
119. R. H. Ball, Gulf General Atomic
120. D. A. Moss, Idaho
121. P. H. Holsted, WADCO
122. D. F. Cope, Oak Ridge National Laboratory
123. C. L. Matthews, Oak Ridge National Laboratory
124. R. L. Philippone, Oak Ridge National Laboratory

AEC-CANOGA PARK AREA OFFICE

125. C. W. Richards

AEC-IDAHO NUCLEAR CORPORATION

126. K. K. Kennedy

AERE, Harwell, England

127. J.D.L. Harrison
128. T. L. Markin
129. P. E. Potter
130. M. H. Rand

AEROJET GENERAL CORPORATION, P. O. Box 15847, Sacramento, Calif. 95801

131. S. G. Harbison

ALLIED CHEMICAL NUCLEAR PRODUCTS, INC., P. O. Box 35, Florham Park, New Jersey 07932

132. R. I. Newman
133. E. M. Shank

ARGONNE NATIONAL LABORATORY

134. J. E. Ayer
135. N. A. Javed
136. J.T.A. Roberts
137. P. G. Shewman
138. R. J. Thorn
139. R. C. Vogel
140. G. H. Winslow
141. Report Section, 203-CE-125
142. LMFBR Program Office

ATCOR, INC., 5 Westchester Plaza, Elmsford, New York 10523

143. Lois Seulowitz

ATLANTIC RICHFIELD HANFORD COMPANY, P. O. Box 250, Richland, Washington 99352

144. W. P. McCue

ATOMIC ENERGY OF CANADA, LTD., Chalk River, Ontario

145. J.A.L. Robertson

ATOMICS INTERNATIONAL

146. Simcha Golan

BABCOCK AND WILCOX COMPANY, Lynchburg, Virginia 24505

147. J. M. Kerr

BROOKHAVEN NATIONAL LABORATORY, Upton, New York 11973

148. E. E. Winche

CENTRE d'ETUDES NUCLEAIRES, Fontenay-aux-Roses, France

149. R. Pascard

CENTRE d'ETUDES NUCLEAIRES, Grenoble, France

150. J. M. Martin

COMBUSTION ENGINEERING, Windsor, Conn. 06095

151. W. P. Staker

SAVANNAH RIVER LABORATORY

152. L. H. Meyer

EUROPEAN INSTITUTE FOR TRANSURANIUM ELEMENTS, Karlsruhe, Germany

153. V. Benedict
154. H. Blank
155. C. Sari

FIAT, SEZIONE ENERGIA NUCLEARE, Torino, Italy

156. R. L. Colombo

GENERAL ELECTRIC, Pleasanton

157. E. A. Aitken

GENERAL ELECTRIC, San Jose

158. R. G. Barnes

GENERAL ELECTRIC, KNOLLS ATOMIC POWER LABORATORY, P. O. Box 1072, Schenectady, New York 12301

159. R. A. Proebstel

GENERAL ELECTRIC, Schenectady, New York 12301

160. R. E. Carter
161. K. W. Lay

GENERAL ELECTRIC, Sunnyvale

162. W. E. Bailey

GULF GENERAL ATOMIC

163. J. Lindgren
164. R. E. Norman
165. K. P. Steward
166. Sidney Strausberg

IDAHO NUCLEAR CORPORATION

167. J. A. Buckham

INTERNATIONAL ATOMIC ENERGY AGENCY, Vienna, Austria

168. Library

JAPAN ATOMIC ENERGY RESEARCH INSTITUTE, Tokai, Japan

169. J. Abe
170. M. Kurihara
171. Library

KERR-McGEE CORPORATION, Oklahoma City, Oklahoma 73102

172. R. M. Fryar

LOS ALAMOS SCIENTIFIC LABORATORY

173. R. Benz
174. E. K. Storms

MASSACHUSETTS INSTITUTE OF TECHNOLOGY, Cambridge, Mass. 02139

175. Manson Benedict
176. E. A. Mason

NATIONAL LEAD COMPANY OF OHIO, Cincinnati

177. S. Marshall

NATIONAL LEAD COMPANY, 111 Broadway, New York, N. Y. 10006

178. S. H. Brown

NORTH AMERICAN CARBON, INC., P. O. Box 19737, Columbus, Ohio 43219

179. J. L. Kovach

NUCLEAR FUEL SERVICES, INC., Wheaton Plaza, Wheaton, Maryland 20902

180. W. H. Lewis

NUCLEAR MATERIALS AND EQUIPMENT CORPORATION, Apollo, Pennsylvania 15613

181. C. S. Caldwell

PENNSYLVANIA STATE UNIVERSITY, MATERIALS RESEARCH LABORATORY, University Park, Pa. 16802

182. K. E. Spear

TOKYO INSTITUTE OF TECHNOLOGY, RESEARCH LABORATORY OF NUCLEAR REACTOR, Tokyo, 152, Japan

183. H. Suzuki

UNITED NUCLEAR CORPORATION, Elmsford, New York 10523

184. A. Strasser

UNIVERSITY OF FLORIDA, DEPARTMENT OF METALLURGICAL AND MATERIALS ENGINEERING, Gainesville, Fla. 32601

185. R. T. DeHoff
186. F. N. Rhines

WADCO, P. O. Box 1970, Richland, Washington 99352

187. R. E. Bardsley
188. W. Devine, Jr.
189. J. P. Keenan
190. W. E. Roake
191. J. Shirley
192. E. T. Weber

WESTINGHOUSE, ADVANCED REACTOR DIVISION, Waltz Mill Site

193. M. G. Bale
194. W. R. Jacoby
195. Peter Murray

WESTINGHOUSE, Pittsburgh

196. R. E. Olson

OAK RIDGE OPERATIONS OFFICE

197. Laboratory and University Division

198–199. Division of Technical Information Extension